Multi-Band, Wide-Beam, Circularly Polarized, Crossed, Asymmetrically Barbed Dipole Antennas for GPS Applications

Son Xuat Ta, Hosung Choo, Ikmo Park, and Richard W. Ziolkowski

***Abstract*—This communication presents a multi-band, circularly polarized (CP), wide beamwidth, highly efficient antenna for use in global positioning systems (GPS). The primary radiating elements are two crossed printed dipoles, which incorporate a 90° phase delay line realized with a vacant-quarter printed ring to produce the CP radiation and broadband impedance matching. To achieve multiple resonances, each dipole arm is divided into four branches with different lengths, and a printed inductor with a barbed end is inserted in each branch to reduce the radiator size. An inverted, pyramidal, cavity-backed reflector is incorporated with the crossed dipoles to produce a unidirectional radiation pattern with a wide 3-dB axial ratio (AR) beamwidth and a high front-to-back ratio. The multi-band antennas have broad impedance matching and 3-dB AR bandwidths, which cover the GPS L1–L5 bands.**

***Index Terms*—Antenna, cavity-backed reflector, circular polarization, global positioning system, multi-band operations, wide-beam radiation.**

I. Introduction

It is well known that circularly polarized (CP) radiation reduces multipath effects and provides flexibility in the orientation angle between transmitting and receiving antennas. Consequently, CP antennas have been applied in many wireless applications, such as global positioning systems (GPS), satellite communication systems, radio frequency identification systems, and wireless local area networks. CP radiation is traditionally generated from two orthogonal currents that have a 90° phase difference. Based on this generation technique, broadband CP antennas that are constructed as two crossed dipoles of equal amplitude and are excited with a 90° phase difference have been reported [1]–[6]. However, these antennas are bulky because they use straight or bowtie dipoles. Crossed-dipole shapes were recently employed as the primary radiating elements of near-field resonant parasitic antennas [7]–[10] in order to achieve CP radiation with compact sizes. Furthermore, microstrip (MS) antennas with CP radiation [11], [12], which were obtained by exciting two orthogonal modes with the requisite 90° time-phase difference between them, have been introduced.

CP radiation is generally adopted in GPS and satellite communications because their signals display less sensitivity between the satellite and ground station when they pass through the ionosphere. All GPS satellites conventionally operate in the same two frequency bands, i.e., L1 (1.57542 GHz) and L2 (1.2276 GHz). Recently, GPS L3 (1.38105 GHz), L4 (1.379913 GHz), and L5 (1.17645 GHz) bands have been added for special applications (e.g., nuclear detonation detection, additional ionospheric correction, and civilian safety-of-life signal reception). Thus, a GPS receiver antenna with right-hand circular polarization (RHCP) preferably has multi-band operation, broad impedance and 3-dB axial ratio (AR) bandwidths, and a wide beam that may be directed toward the sky [13]. Various kinds of antennas with single-feed and CP radiation have been presented for the GPS L1 and L2 bands, including a multilayer substrate MS antenna [14], [15], MS-fed slotted antennas [16], [17], and stacked patch antennas [18]–[20]. Recently, a single-feed, stacked, patch CP antenna was introduced for triple-band GPS receivers [21]. Most of the abovementioned antennas, however, concentrate on CP generation and 3-dB AR bandwidth enhancement rather than any improvement of the 3-dB AR beamwidth. On the other hand, a pyramidal ground structure with a partially enclosed, flat, conducting wall has been adopted in order to increase the beamwidth of the CP radiation [11]. Unfortunately, the overall design configuration is unwieldy because of the complexity of the prototype ground structure. A technique for extending the substrate beyond the ground plane was introduced for a dual-frequency patch antenna in order to realize a wide CP radiation beamwidth [22]. However, this technique could be accompanied by an increase in surface waves, and its 3-dB AR bandwidth is insufficient for some applications.

In this communication we describe a multi-band, RHCP, crossed, multi-branch, barbed dipole antenna with a broad impedance-matching bandwidth, and a high front-to-back ratio in the GPS L1–L5 bands. The multi-branch barbed dipole with a meander line in each branch is used to achieve not only multiple resonances but also a significant reduction in the radiator size. A vacant-quarter printed ring is used as a 90° phase delay line to generate the CP radiation [23], [24]. The crossed multi-branch dipoles are backed by an inverted pyramidal cavity to provide wide-beam radiation, a high front-to-back ratio, and a similar gain in the GPS L1–L5 bands. The antenna characteristics were investigated using an ANSYS high-frequency structure simulator (HFSS) and were validated by experiment.

II. Antenna Geometry and Design

Fig. 1 shows the geometry of the multi-band CP antenna. The antenna is composed of two printed dipoles, a coaxial line, and a reflector. The reflector is an inverted pyramidal cavity with a rectangular bottom measuring 120 × 120 mm, a top aperture measuring 160 × 160 mm, and a height of 40 mm. The coaxial line is punctured through the bottom of the cavity to excite the radiator. The dipoles are printed on both sides of a 62 × 62 mm Rogers RO4003 substrate with a relative permittivity of 3.38, a loss tangent of 0.0027, and a thickness of 0.508 mm. The outer conductor of the coaxial line is connected to the arms on the bottom side of the substrate. The inner conductor of the coaxial line extends through the substrate and connects to the arms on the top side. Each dipole arm is divided into four branches, each of which has a meander line with a barbed end, and each branch is distinctly designed to operate in the GPS L5, L2, L3/4, and L1 bands. The n^{th} ($n = 1$ to 4) meander line starts at L_{bn} from the center with a trace width $w_{\rm in}$, and its segments have a gap size of $g_{\rm in}$ and length of $L_{\rm in}$. The dipoles are crossed through a vacant-quarter printed ring that acts as a 90° phase delay line to obtain the desired CP radiation.

For the initial design of the proposed antenna, asymmetrically barbed arrowhead dipoles [24] were first designed in free space in order to provide resonances in the GPS L1 and L2 bands and then crossed through a 90° phase delay line realized by a vacant-quarter printed ring in order to produce the CP radiation. The crossed dipoles are equipped with a cavity-backed reflector to provide a unidirectional radiation pattern with a wide AR beamwidth and a high front-to-back ratio in both bands. In order to generate more resonances, two other branches with different lengths were added to the arm of the asym-

Manuscript received December 05, 2012; revised April 01, 2013; accepted July 30, 2013. Date of publication August 16, 2013; date of current version October 28, 2013.

S. X. Ta and I. Park are with the Department of Electrical and Computer Engineering, Ajou University, Suwon 443-749, Korea (e-mail: tasonxuat@ajou.ac.kr, ipark@ajou.ac.kr).

H. Choo is with the School of Electronics and Electrical Engineering, Hongik University, Seoul 121-791 Korea (e-mail: hschoo@hongik.ac.kr).

R. W. Ziolkowski is with the Department of Electrical and Computer Engineering University of Arizona, Tucson, AZ 85721 USA (e-mail: ziolkowski@ece.arizona.edu).

Color versions of one or more of the figures in this communication are available online at http://ieeexplore.ieee.org.

Digital Object Identifier 10.1109/TAP.2013.2277915

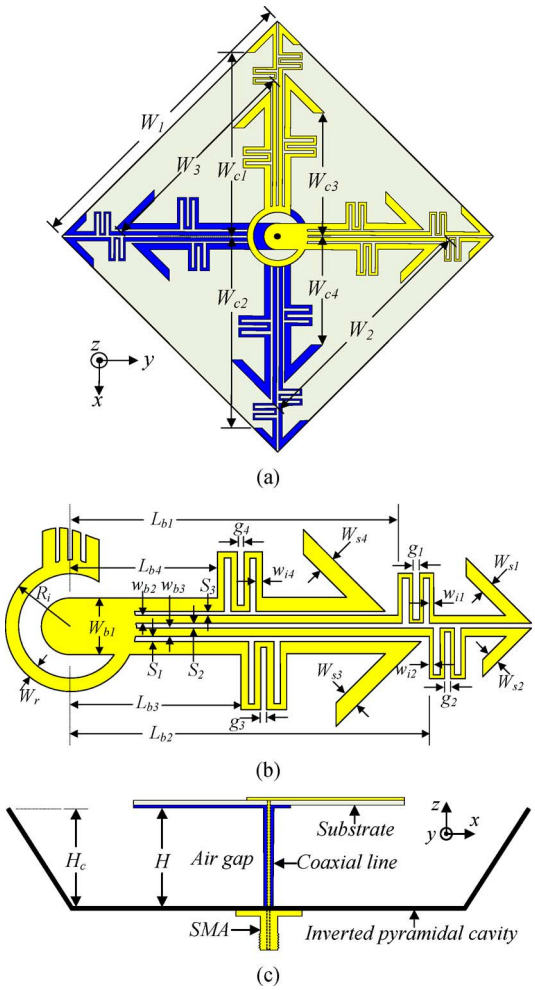

Fig. 1. Geometry of the crossed, multi-branch, asymmetrically barbed dipole antenna: (a) radiator, (b) vacant-quarter printed ring and dipole arm, and (c) side view with the inverted pyramidal cavity.

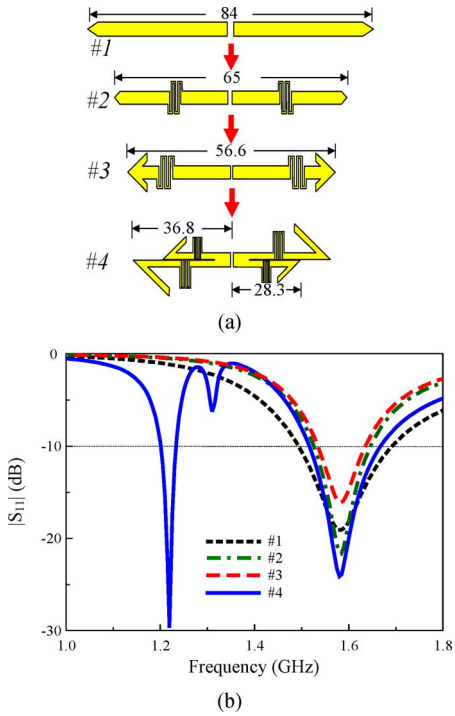

Fig. 2. Asymmetrically barbed arrowhead dipole design process. (a) Basic designs (units in mm), and (b) their simulated $|S_{11}|$ values as a function of the frequency.

metrically barbed arrowhead dipole. Thus, the design is referred to as a multi-branch asymmetrically barbed dipole. A conventional rectangular cavity, which is introduced to enhance the radiation characteristics of an antenna, was modified to become an inverted pyramidal cavity. This design allowed us to achieve a similar gain in all of the GPS L1–L5 bands. Optimized antenna design parameters were determined to obtain CP radiation and multi-band operations that covers all of the GPS L1–L5 bands. These parameters are as follows: $W_1 = 62$ mm, $W_2 = 50$ mm, $W_3 = 42$ mm, $W_{c1} = 38$ mm, $W_{c2} = 39$ mm, $W_{c3} = 25$ mm, $W_{c4} = 22.5$ mm, $R_i = 6.2$ mm, $W_r = 1.2$ mm, $w_{s1} = w_{s2} = 1.2$ mm, $w_{s3} = w_{s4} = 1.6$ mm, $L_{b1} = 30.4$ mm, $w_{i1} = 0.4$ mm, $g_{i1} = 0.6$ mm, $L_{i1} = 5$ mm, $L_{b2} = 34$ mm, $w_{i2} = 0.4$ mm, $g_{i2} = 0.6$ mm, $L_{i2} = 5$ mm, $L_{b3} = 16$ mm, $w_{i3} = 0.6$ mm, $g_{i3} = 0.6$ mm, $L_{i3} = 7.8$ mm, $L_{b4} = 14$ mm, $w_{i4} = 0.4$ mm, $g_{i4} = 0.6$ mm, $L_{i4} = 7.8$ mm, $W_{b1} = 5.6$ mm, $W_{b2} = W_{b3} = 0.8$ mm, $S_1 = S_2 = S_3 = 0.4$ mm, $H_c = 40$ mm, and $H = 40$ mm.

A. Design of Crossed Asymmetrically Barbed Arrowhead Dipoles in Free Space

In order to reduce the sizes of the primary radiating elements, the proposed antenna uses two techniques: the insertion of printed inductors in each dipole arm and an arrowhead-shaped trace at its end. The process of length reduction is illustrated in Fig. 2(a). The initial design, termed the #1 dipole, was a printed straight dipole operating at the GPS L1 band, with a length, width, and feed gap equal to 84 mm ($\sim 0.44\ \lambda_0$), 4 mm, and 1 mm, respectively. The dipole was arranged on a diagonal of a $59.4 \times 59.4\ \text{mm}^2$ piece of the Rogers RO4003 substrate. The #1 dipole was simulated assuming a $Z_0 = 50\ \Omega$ excitation source; it yielded a resonance at 1.58 GHz with $|S_{11}| = -19.1$ dB (Fig. 2(b)).

In order to reduce its length but keep the same resonance, two printed inductors were symmetrically inserted into the arms of the original #1 dipole; this design is denoted as the #2 dipole. While it has the same resonance frequency, the #2 dipole has a much shorter length, 65 mm ($\sim 0.34\ \lambda_0$), and a subsequent narrower bandwidth compared to the corresponding values of the #1 dipole. From the reflection coefficient formula, $\Gamma = (Z_{in} - Z_0)/(Z_{in} + Z_0)$, the input impedance, Z_{in}, of the dipole is reduced with a decrease in the dipole length and can be increased by inserting the printed inductors, each with an impedance equal to Z_p. Therefore, impedance matching was obtained by adjusting Z_p. The impedance of the printed inductors was adjusted according to the usual principles, i.e., thinner traces and longer meandering line segments produce more inductance, and smaller gaps produce more capacitance. The optimal parameters of the printed inductors of the #2 dipole were a starting point of $L_b = 13$ mm, a trace width of $w_i = 0.6$ mm, and a gap size of $g_i = 0.4$ mm.

To further reduce its length, the ends of the dipole were formed into the shape of an arrowhead; this design is denoted as the #3 dipole. The #3 dipole has a considerably shorter length of 56.6 mm ($\sim 0.298\ \lambda_0$) and a corresponding narrower bandwidth. It has the same resonance frequency as the #2 dipole. The HFSS simulations showed that as the arrowhead increases in size, the resonant frequency decreases. While the desired reduction in the dipole length is attained by introducing the printed inductor and arrowhead-shaped trace, it also is accompanied by a degradation of the impedance-matching bandwidth.

To add another resonance at the GPS L2 band, the #3 dipole was modified by creating an asymmetrically barbed arrowhead. This design, denoted as the #4 dipole, contains two printed inductors and two

TABLE I
ANTENNA PERFORMANCE CHARACTERISTICS FOR DIFFERENT CAVITY-BACKED REFLECTOR HEIGHTS

H_c (mm)	Band name	Resonance frequencies (GHz)	3-dB AR bandwidth (GHz)	CP center frequency (GHz)	Gain at CP center frequency (dBic)	3-dB AR beamwidths (deg.)	
						x-z plane	y-z plane
0	L2	1.223, 1.281	0	1.243	6.32	0°	0°
	L1	1.498, 1.623	1.569–1.626	1.595	7.40	52°	96°
20	L2	1.214, 1.266	1.231–1.246	1.238	6.48	69°	119°
	L1	1.494, 1.600	1.546–1.620	1.579	7.74	98°	115°
40	L2	1.202, 1.255	1.215–1.235	1.227	6.15	144°	143°
	L1	1.485, 1.578	1.530–1.602	1.561	7.48	164°	173°

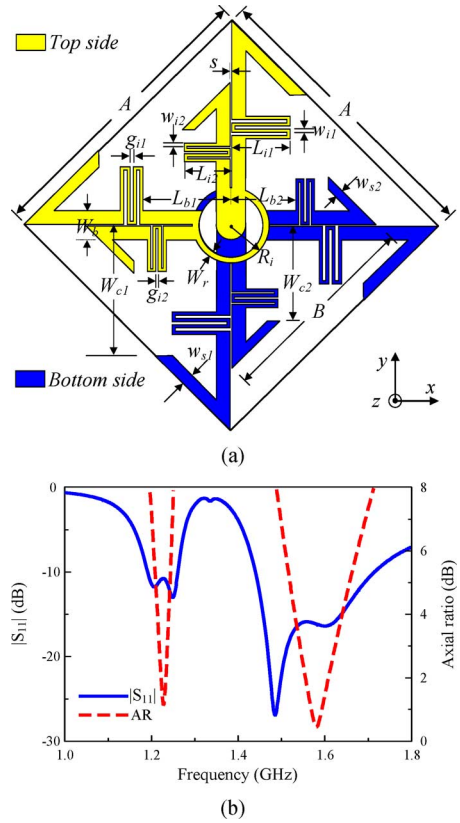

Fig. 3. Dual-band, crossed, asymmetrically barbed arrowhead dipole antenna without the reflector. (a) Design, and (b) its simulated $|S_{11}|$ and AR values.

half-arrowheads of different sizes. The lengths of the small and large branches of the #4 dipole were 56.6 mm (0.298 λ_0 at 1.575 GHz) and 73.6 mm (0.3 λ_0 at 1.227 GHz), respectively. The #4 dipole parameters are the same as those in the fabricated design [24]. As shown in Fig. 2(b), the #4 dipole yielded two main resonances near 1.227 GHz and 1.575 GHz, and an undesired resonance around 1.31 GHz. The undesired resonant frequency is generated by the coupling between the two branches of the dipole arms.

The final design utilizes two #4 dipoles that are crossed on the diagonals of the 52×52 mm^2 substrate in order to produce the desired CP radiation. A vacant-quarter printed ring acts as a 90° phase delay line in order to produce the CP radiation. The crossed asymmetrically barbed arrowhead dipoles without a reflector (Fig. 3(a)) were first examined and then optimized for the desired CP dual-band operation at the GPS L1 and L2 bands. Their parameters are: $A = 54$ mm, $B = 40$, $W_{c1} = 26$ mm, $W_{c2} = 21$ mm, $R_i = 6$ mm, $W_r = 1$ mm, $W_b = 5.4$ mm, $L_{b1} = 17$ mm, $L_{b2} = 13$ mm, $L_{i1} = 10$ mm, $L_{i2} = 8$ mm, $g_{i1} = 0.8$ mm, $w_{i1} = 0.6$ mm, $g_{i2} = 0.6$ mm, $w_{i2} = 0.6$ mm, $W_{s1} = 1.6$ mm, $W_{s2} = 2$ mm, and $S = 0.4$ mm. Fig. 3(b) shows the simulated $|S_{11}|$ and AR values for the crossed dipoles without a reflector. Notice that the impedance matching bandwidth was improved in both bands by the presence of the printed ring. In particular, there are two resonant frequencies around each original resonance, but there are only two CP center frequencies, one at 1.575 GHz and one at 1.227 GHz. The CP center frequency is defined as the frequency at which the AR is at a minimum. The crossed dipole exhibited $|S_{11}| < -10$ dB bandwidths of 1.192–1.261 GHz (69 MHz) and 1.441–1.713 GHz (272 MHz) and the corresponding 3-dB AR bandwidths of 1.219–1.236 GHz (17 MHz) and 1.543–1.624 GHz (81 MHz), respectively. Without a reflector, the crossed, asymmetrically barbed, arrowhead dipole antenna radiates a bidirectional electromagnetic wave; the front-side radiates RHCP, while the back-side radiates left-hand circular polarization (LHCP). One special feature is that the RHCP and LHCP results are interchangeable simply by reversing the vacant-quarter printed ring. The peak gain of the antenna was only 2.1 and 1.32 dBic for the GPS L1 and L2 bands, respectively, due to its small size and the absence of a reflector.

B. Crossed, Asymmetrically Barbed, Arrowhead Dipole Antenna With Cavity-Backed Reflector

In order to improve the radiation characteristics, especially to obtain a high front-to-back ratio and a wide beamwidth, a cavity was introduced as a reflector of the dual-band dipole antenna. The detailed geometry and optimized results of the dual-band antenna were reported in our previous work [24]. To illustrate these cavity-backed improvements, the performance of the dual-band design for different heights (H_c) of the cavity was studied. The corresponding antenna characteristics are summarized in Table I. To better understand the effect of the cavity height on the radiation pattern, the 3-dB AR beamwidth at the CP center frequency for the different H_c values were compared. The proposed antenna exhibited the maximum 3-dB AR beamwidth at the CP center frequency of each operating band. As shown in Table I, with an increase in the cavity height, the antenna gain changed slightly, but the resonance and CP center frequencies of the antenna decreased and the 3-dB AR beamwidth was widened significantly in both operating bands. In addition, the HFSS simulations demonstrated that the antenna with a planar reflector ($H_c = 0$ mm) showed an AR > 3 dB in the lower band and a 3-dB AR beamwidth $< 100°$ in the upper band. $H_c = 20$ mm produced a 3-dB AR beamwidth $< 120°$ in both bands, while $H_c = 40$ mm produced a 3-dB AR beamwidth $> 140°$ and $> 160°$ in the lower and upper bands, respectively. These results indicated that the cavity-backed reflector facilitates the production of wide-beam radiation.

C. Inverted Pyramidal Cavity-Backed Reflector

As mentioned previously, two other branches were added to the arms of the asymmetrically barbed arrowhead dipoles in order to achieve multi-band operation (Fig. 1(b)). The multi-branch asymmetrically barbed dipole antenna was first equipped with a conventional cavity-backed reflector with base dimensions of 120×120 mm^2 and a height of 40 mm. However, the gains for the lower and upper bands differed by more than 1 dB. Moreover, the HFSS simulations indicated

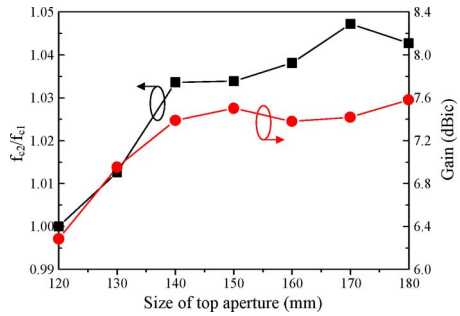

Fig. 4. Simulated f_{c2}/f_{c1} and antenna gain values at the GPS L5 frequency (1.175 GHz) for different top aperture sizes of the inverted pyramidal cavity.

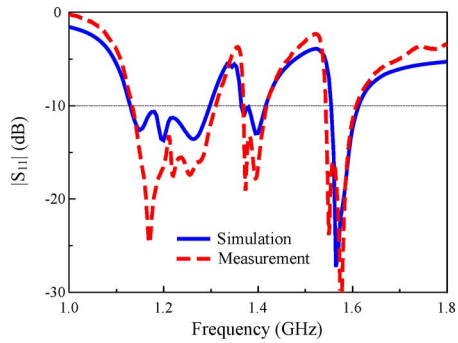

Fig. 5. Simulated and measured reflection coefficients of the multi-band CP antenna.

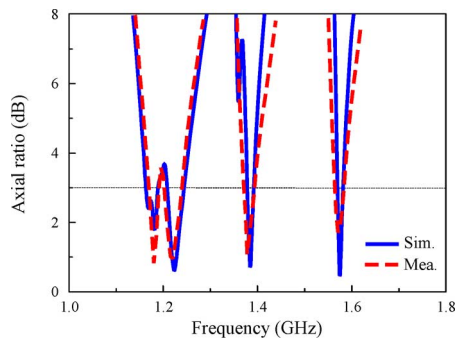

Fig. 6. Simulated and measured ARs of the multi-band GPS antenna.

that the coupling between the two longer branches of the multi-branch dipole arm was significant, as their operating frequencies (GPS L5 and L2 bands) are very close. Therefore, it was relatively difficult to achieve two distinct CP center frequencies for the lower bands with a conventional cavity. In order to solve these problems, the conventional cavity was replaced with an inverted pyramidal cavity. By adjusting the size of the top aperture of the inverted pyramidal cavity, the desired operating frequencies were obtained and the antenna gain in the low frequency band was improved. These features can be seen in Fig. 4, which shows the simulated f_{c2}/f_{c1} ratio and the antenna gain at the GPS L5 frequency (1.175 GHz) for different sizes of the top aperture of the inverted pyramidal cavity while the other parameters are fixed. Here, f_{c1} and f_{c2} are the CP center frequencies for the first and second bands, respectively, of the multi-band antenna. As shown in Fig. 4, the size of the top aperture varies from 120 mm to 180 mm in 10-mm steps, and the f_{c2}/f_{c1} ratio and gain increase. The antenna with a conventional cavity-backed reflector (with a top aperture size of 120 mm) yields $f_{c1} = f_{c2}$ and a gain of 6.35 dBic at 1.175 GHz. With a top aperture size of 160 mm, the ratio f_{c2}/f_{c1} is approximately equal to the GPS L2 over the L5 frequency ratio with a gain of 7.42 dBic at 1.175 GHz. In addition, the HFSS simulations showed that a value of 160 mm offers optimized results in terms of a broad 3-dB AR bandwidth for the first and second bands. The effect of the size of the top aperture on the antenna's performance in higher bands is negligible and is not shown here.

III. Measurements

The proposed pyramidal cavity-backed, crossed, multi-branch, asymmetrically barbed dipole antenna was fabricated and measured. The primary radiating element was built on both sides of a Rogers RO4003 substrate with a copper thickness of 20 μm, via a standard etching technology. The inverted pyramidal cavity was constructed from five copper plates with a thickness of 0.2 mm. Fig. 5 presents a comparison between the measured and simulated reflection coefficients for this antenna. The measured impedance bandwidths for a -10 dB reflection coefficient were 1.131–1.312 GHz (181 MHz), 1.369–1.421 GHz (52 MHz), and 1.543–1.610 GHz (67 MHz), which are in agreement with the simulated bandwidths of 1.130–1.295 GHz (165 MHz), 1.365–1.415 GHz (50 MHz), and 1.556–1.610 GHz (54 MHz), respectively. Fig. 6 presents the simulated and measured AR of the antenna, which show similar results. The measured 3-dB AR bandwidths were 1.165–1.190 GHz (25 MHz), 1.195–1.240 GHz (45 MHz), 1.370–1.395 GHz (25 MHz), and 1.565–1.585 GHz (20 MHz), whereas the simulated 3-dB AR bandwidths were 1.163–1.189 GHz (26 MHz), 1.208–1.244 GHz (36 MHz), 1.378–1.392 GHz (14 MHz), and 1.569–1.582 GHz (13 MHz), respectively. The measurements yielded CP center frequencies for the four bands of 1.175, 1.225, 1.380, and 1.575 GHz with ARs of 0.83, 0.96, 0.94, and 1.4 dB, respectively.

The radiation patterns of the proposed multi-band antenna at 1.175, 1.225, 1.380, and 1.575 GHz are presented in Fig. 7 and show good agreement between the measurements and the simulations. The radiation was RHCP and symmetric in both the x–z and the y–z planes. At 1.175 GHz, the measurements yielded a gain of 7.55 dBic, a front-to-back ratio of 24 dB, half-power beamwidths (HPBWs) of 100° and 102° in the x–z and y–z planes, respectively, and 3-dB AR beamwidths of 161° and 120° in the x–z and y–z planes, respectively. At 1.225 GHz, the measurements yielded a gain of 7.7 dBic, a front-to-back ratio of 26 dB, HPBWs of 100° and 102° in the x–z and y–z planes, respectively, and 3-dB AR beamwidths of 112° and 134° in the x–z and y–z planes, respectively. At 1.380 GHz, the measurements yielded a gain of 8.1 dBic, a front-to-back ratio of 25 dB, HPBWs of 105° and 103° in the x–z and y–z planes, respectively, and 3-dB AR beamwidths of 124° and 145° in the x–z and y–z planes, respectively. At 1.575 GHz, the measurements yielded a gain of 7.94 dBic, a front-to-back ratio of 27 dB, HPBWs of 90° and 96° in the x–z and y–z planes, respectively, and 3-dB AR beamwidths of 168° and 135° in the x–z and y–z planes, respectively. In addition, the measurements resulted in high radiation efficiencies, which were 87.63%, 88.96%, 90.69%, and 91.73% at 1.175 GHz, 1.225 GHz, 1.380 GHz, and 1.575 GHz, respectively.

IV. Conclusion

We introduce a crossed, multi-branch, asymmetrically barbed, dipole CP antenna incorporated with a cavity-backed reflector for multi-band GPS applications. To achieve multi-resonances, the branches were designed with different lengths. A meander line with a barb was inserted in each branch to reduce the radiator size. To generate CP radiation, a vacant-quarter printed ring with broadband impedance matching was used as the 90° phase delay line. The replacement of a conventional

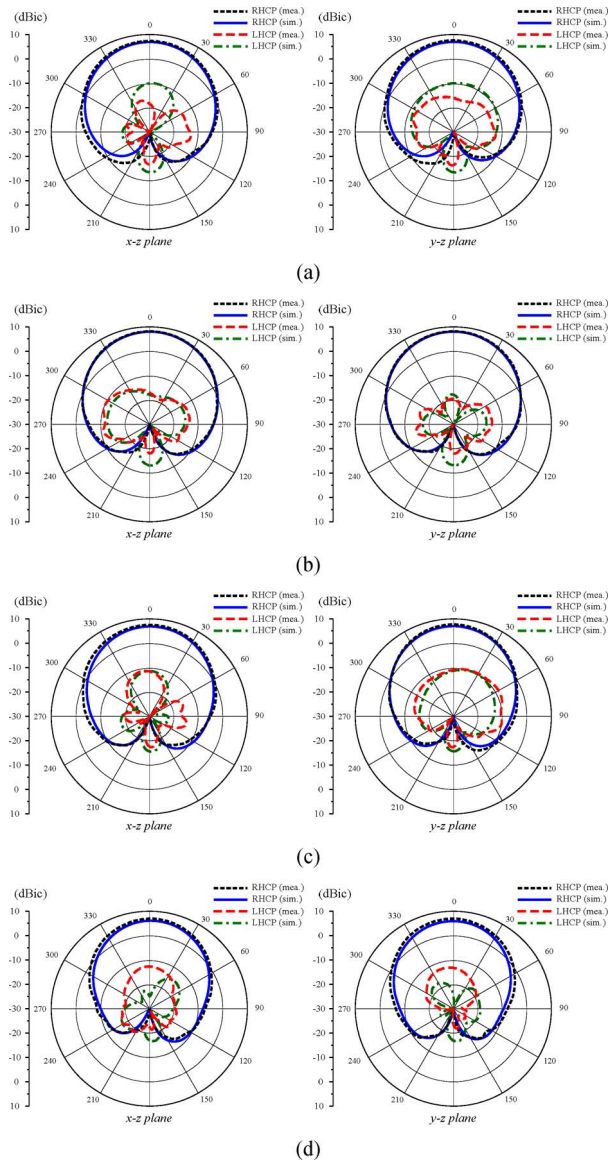

Fig. 7. Radiation patterns of the antenna at (a) 1.175 GHz, (b) 1.225 GHz, (c) 1.380 GHz, and (d) 1.575 GHz.

reflector by an inverted pyramidal cavity reflector improved the radiation patterns, yielding wide beamwidths and high front-to-back ratios. The proposed antenna has bandwidths of 1.131–1.312 GHz (181 MHz), 1.369–1.421 GHz (52 MHz), and 1.543–1.610 GHz (67 MHz) for impedance matching with $|S_{11}| < -10$ dB and 1.165–1.190 GHz (25 MHz), 1.195–1.240 GHz (45 MHz), 1.370–1.395 GHz (25 MHz), and 1.565–1.585 GHz (20 MHz) for an AR of < 3 dB. In addition, the antenna has a wide beamwidth ($> 90^\circ$ for the HPBW and $> 110^\circ$ for the 3-dB AR beamwidth), high radiation efficiency ($> 85\%$), and a high front-to-back ratio (> 18 dB). With their many advantages, these antennas can be widely applied to GPS as well as to satellite communication applications.

REFERENCES

[1] J. W. Baik, K. J. Lee, W. S. Yoon, T. H. Lee, and Y. S. Kim, "Circular polarized printed crossed dipole antennas with broadband axial ratio," *Electron. Lett.*, vol. 44, no. 13, pp. 785–786, Jun. 2008.

[2] K. Mak and K. Luk, "A circularly polarized antenna with wide axial ratio beamwidth," *IEEE Trans. Antennas Propag.*, vol. 57, no. 10, pp. 3309–3312, Oct. 2009.

[3] S. Qu, C. Chan, and Q. Xue, "Wideband and high-gain composite cavity-backed crossed triangular bowtie dipoles for circular polarized radiation," *IEEE Trans. Antennas Propag.*, vol. 58, no. 10, pp. 3157–3164, Oct. 2010.

[4] J. W. Baik, T. H. Lee, S. Pyo, S. M. Han, J. Jeong, and Y. S. Kim, "Broadband circularly crossed dipole with parasitic loop resonators and its array," *IEEE Trans. Antennas Propag.*, vol. 59, no. 1, pp. 80–88, Jan. 2011.

[5] L. Wang, H. Yang, and Y. Li, "Design of a new printed dipole antenna using in high latitudes for Inmarsat," *IEEE Antennas Wireless Propag. Lett.*, vol. 10, pp. 358–360, 2011.

[6] J. Zhang, H. Yang, and D. Yang, "Design of a high-gain circularly polarized antenna for Inmarsat Communications," *IEEE Antennas Wireless Propag. Lett.*, vol. 11, pp. 350–353, 2012.

[7] C. Lin, P. Jin, and R. W. Ziolkowski, "Multi-functional, magnetically-coupled, electrically small, near-field resonant parasitic wire antennas," *IEEE Trans. Antennas Propag.*, vol. 59, no. 3, pp. 714–724, Mar. 2011.

[8] P. Jin and R. W. Ziolkowski, "Multi-frequency, linear and circular polarized, metamaterial-inspired, near-field resonant parasitic antennas," *IEEE Trans. Antennas Propag.*, vol. 59, no. 5, pp. 1446–1459, May 2011.

[9] P. Jin, C. Lin, and R. W. Ziolkowski, "Multifunctional, electrically small, planar near-field resonant parasitic antennas," *IEEE Antennas Wireless Propag. Lett.*, vol. 11, pp. 200–204, 2012.

[10] P. Jin and R. W. Ziolkowski, "High directivity, electrically small, low-profile, near-field resonant parasitic antennas," *IEEE Antennas Wireless Propag. Lett.*, vol. 11, pp. 305–309, 2012.

[11] C. W. Su, S. K. Huang, and C. H. Lee, "CP microstrip antenna with wide beamwidth for GPS band application," *Electron. Lett.*, vol. 43, no. 20, pp. 1062–1063, Sep. 2007.

[12] K. Lam, K. Luk, K. Lee, H. Wong, and K. Ng, "Small circularly polarized U-slot wideband patch antenna," *IEEE Antennas Wireless Propag. Lett.*, vol. 10, pp. 87–90, 2011.

[13] J. J. H. Wang, "Antennas for Global Navigation Satellite System (GNSS)," *Proc. IEEE*, vol. 100, no. 7, pp. 2349–2355, Jul. 2012.

[14] L. Boccia, G. Amendola, and G. Massa, "A dual frequency microstrip patch antenna for high-precision GPS applications," *IEEE Antennas Wireless Propag. Lett.*, vol. 3, pp. 157–160, 2004.

[15] S. Chen, G. Liu, X. Chen, T. Lin, X. Liu, and Z. Duan, "Compact dual-band GPS microstrip antenna using multilayer LTCC substrate," *IEEE Antennas Wireless Propag. Lett.*, vol. 9, pp. 421–423, 2010.

[16] Nasimuddin, Z. Chen, and X. Qing, "Dual-band circularly polarized S-shaped slotted patch antenna with a small frequency ratio," *IEEE Trans. Antennas Propag.*, vol. 58, no. 6, pp. 2112–2115, Jun. 2010.

[17] W. Hsieh, T. Chang, and J. Kiang, "Dual-band circularly polarized cavity-backed annular slot antenna for GPS receiver," *IEEE Trans. Antennas Propag.*, vol. 60, no. 4, pp. 2076–2080, Apr. 2012.

[18] Z. Wang, S. Fang, S. Fu, and S. Lu, "Dual-band probe-fed stacked patch antenna for GNSS applications," *IEEE Antennas Wireless Propag. Lett.*, vol. 8, pp. 100–103, 2009.

[19] X. Sun, Z. Zhang, and Z. Feng, "Dual-band circularly polarized stacked annular-ring patch antenna for GPS application," *IEEE Antennas Wireless Propag. Lett.*, vol. 10, pp. 49–52, 2011.

[20] D. Li, P. Guo, Q. Dai, and Y. Fu, "Broadband capacitively coupled stacked patch antenna for GNSS applications," *IEEE Antennas Wireless Propag. Lett.*, vol. 11, pp. 701–704, 2012.

[21] O. Falade, M. Rehman, Y. Gao, X. Chen, and C. Parini, "Single feed stacked patch circular polarized antenna for triple band GPS receivers," *IEEE Trans. Antennas Propag.*, vol. 60, no. 10, pp. 4479–4484, Oct. 2012.

[22] X. L. Bao and M. J. Ammann, "Dual-frequency dual circularly-polarised patch antenna with wide beamwidth," *Electron. Lett.*, vol. 44, no. 21, pp. 1233–1234, Oct. 2008.

[23] S. X. Ta, J. J. Han, and I. Park, "Compact circularly polarized composite cavity-backed crossed dipole for GPS applications," *J. Electromag. Eng. Sci.*, vol. 13, no. 1, pp. 44–49, Mar. 2013.

[24] S. X. Ta, I. Park, and R. W. Ziolkowski, "Dual-band wide-beam crossed asymmetric dipole antenna for GPS application," *Electron. Lett.*, vol. 48, no. 25, pp. 1580–1581, Dec. 2012.